REPORT DOCUMENTATION PAGE

Form Approved OMB NO. 0704-0188

1. REPORT DATE (DD-MM-YYYY)	2. REPORT TYPE	3. DATES COVERED (From - To)
	New Reprint	-

4. TITLE AND SUBTITLE
Light-hole and heavy-hole transitions for high-temperature long-wavelength infrared detection

5a. CONTRACT NUMBER
W911NF-08-1-0448

5b. GRANT NUMBER

5c. PROGRAM ELEMENT NUMBER
611102

6. AUTHORS
Y. F. Lao, P. K. D. D. P. Pitigala, A. G. U. Perera, H. C. Liu, M. Buchanan, Z. R. Wasilewski, K. K. Choi, P. Wijewarnasuriya

5d. PROJECT NUMBER

5e. TASK NUMBER

5f. WORK UNIT NUMBER

7. PERFORMING ORGANIZATION NAMES AND ADDRESSES
Georgia State University
Office of Sponsored Programs
Georgia State University Research Foundation, Inc.
Atlanta, GA 30302 -3999

8. PERFORMING ORGANIZATION REPORT NUMBER

9. SPONSORING/MONITORING AGENCY NAME(S) AND ADDRESS(ES)
U.S. Army Research Office
P.O. Box 12211
Research Triangle Park, NC 27709-2211

10. SPONSOR/MONITOR'S ACRONYM(S)
ARO

11. SPONSOR/MONITOR'S REPORT NUMBER(S)
54109-EL.3

12. DISTRIBUTION AVAILIBILITY STATEMENT
Approved for public release; distribution is unlimited.

13. SUPPLEMENTARY NOTES
The views, opinions and/or findings contained in this report are those of the author(s) and should not contrued as an official Department of the Army position, policy or decision, unless so designated by other documentation.

14. ABSTRACT
Hole transitions from the heavy-hole (hh) to the light-hole (lh) band contributing to the 4–10??m response range are reported on p-GaAs/AlGaAs detectors. The detectors show a spectral response up to 16.5??m, operating up to a temperature of 330 K where the lh-hh response is superimposed on the free-carrier response. Two characteristic peaks observed between 5–7??m are in good agreement with corresponding energy separations of the lh and hh bands and thus originated from lh-hh transitions. Results will be useful for designing multi-spectral detection which

15. SUBJECT TERMS
aluminium compounds, energy gap, gallium arsenide, III-V semiconductors, infrared detectors

16. SECURITY CLASSIFICATION OF:			17. LIMITATION OF ABSTRACT	15. NUMBER OF PAGES	19a. NAME OF RESPONSIBLE PERSON
a. REPORT	b. ABSTRACT	c. THIS PAGE			Unil Perera
UU	UU	UU	UU		19b. TELEPHONE NUMBER: 404-413-6037

Report Title

Light-hole and heavy-hole transitions for high-temperature long-wavelength infrared detection

ABSTRACT

Hole transitions from the heavy-hole (hh) to the light-hole (lh) band contributing to the 4–10??m response range are reported on p-GaAs/AlGaAs detectors. The detectors show a spectral response up to 16.5??m, operating up to a temperature of 330 K where the lh-hh response is superimposed on the free-carrier response. Two characteristic peaks observed between 5–7??m are in good agreement with corresponding energy separations of the lh and hh bands and thus originated from lh-hh transitions. Results will be useful for designing multi-spectral detection which could be realized on a single p-GaAs structure.

REPORT DOCUMENTATION PAGE (SF298)
(Continuation Sheet)

Continuation for Block 13

ARO Report Number 54109.3-EL
Light-hole and heavy-hole transitions for high-te ...

Block 13: Supplementary Note

Approved for public release; distribution is unlimited.

Light-hole and heavy-hole transitions for high-temperature long-wavelength infrared detection

Y. F. Lao,[1] P. K. D. D. P. Pitigala,[1] A. G. U. Perera,[1,a)] H. C. Liu,[2] M. Buchanan,[2] Z. R. Wasilewski,[2] K. K. Choi,[3] and P. Wijewarnasuriya[3]
[1]*Department of Physics and Astronomy, Georgia State University, Atlanta, Georgia 30303, USA*
[2]*Institute for Microstructural Sciences, National Research Council, Ottawa, Ontario K1A 0R6, Canada*
[3]*U.S. Army Research Laboratory, Adelphi, Maryland 20783-1197, USA*

(Received 15 June 2010; accepted 16 August 2010; published online 2 September 2010)

Hole transitions from the heavy-hole (*hh*) to the light-hole (*lh*) band contributing to the 4–10 μm response range are reported on *p*-GaAs/AlGaAs detectors. The detectors show a spectral response up to 16.5 μm, operating up to a temperature of 330 K where the *lh-hh* response is superimposed on the free-carrier response. Two characteristic peaks observed between 5–7 μm are in good agreement with corresponding energy separations of the *lh* and *hh* bands and thus originated from *lh-hh* transitions. Results will be useful for designing multi-spectral detection which could be realized on a single *p*-GaAs structure. © *2010 American Institute of Physics*.
[doi:10.1063/1.3486169]

Recently, uncooled 3–5 μm detectors based on hole transitions from the light/heavy hole (*lh*/*hh*) bands to the spin-orbit split-off (*so*) band were reported[1,2] using *p*-GaAs/AlGaAs structures. This mechanism can provide an extended spectral range by varying the materials with different *so* splitting energies (Δ_{so}). For example, III-V phosphide material will allow 8–14 μm detection (e.g., Δ_{so}(GaP) =0.08 eV). As a result of spin-orbit interaction, the *lh* and *hh* bands are also separated with an energy approximately approaching $(2/3)\Delta_{so}$ at wave vectors (k) away from the Brillouin Zone (BZ) center. Hole transitions between these two bands can lead to optical absorption at wavelengths up to 10 μm for *p*-GaAs.[3] In this letter, attention is paid to spectral response due to *lh-hh* transitions in *p*-GaAs/AlGaAs detectors, showing attractive applications for mid- and long-wavelength infrared (MWIR and LWIR) detection.

Research on MWIR and LWIR detectors such as mercury-cadmium telluride (MCT),[4] quantum-well and dot infrared photodetectors (QWIP[5] and QDIP[6]), type-II InAs/GaSb strained layer superlattice (SLS)[7] and quantum cascade detectors (QCD)[8] is still in progress, wherein uniformity, low cost, and multispectral detection are desirable for practical applications. As a mature material system, GaAs is such a candidate. The detectors demonstrated here have a similar structure to the standard[9] heterojunction interfacial work-function internal photoemission detector which consists of alternative highly *p*-doped absorbing layers (emitters) and undoped barriers. The highly doped and thick emitters (18.8 nm) will lead to three-dimensional energy states as opposed to quantized states. Carriers excited by incoming radiation in a split-off detector[1,2] originate from hole transitions taking place either between different bands (intervalence-band absorption, IVBA), specifically from the *hh* band to the *so* band, or within the same band (free-carrier absorption, FCA). These carriers then escape over the barriers by a photoemission process occurring at the emitter-barrier interface. The internal work function is defined by energy difference between the barrier bottom and the Fermi level (or the valence-band edge if the Fermi level is above it) of emitters, and determines the threshold wavelength (λ_t). The spectral limitation comes from the requirement of photon-energy greater than Δ_{so}, e.g., 0.341 eV for GaAs. On the contrary, *lh-hh* transition energy has a high onset due to their maximum separation $\Delta_1(\Lambda)$ (Refs. 10 and 11) in the $\langle 111\rangle(\Lambda)$ direction, but no minimum limitation from the band-structure point of view. Therefore, *lh-hh* transitions can theoretically produce broad absorption features up to the wavelength region where FCA becomes dominating.

The detailed valence-band structure of GaAs is shown in Fig. 1(a) to illustrate various IVBA processes. Three types of hole transitions, i.e., from $hh \rightarrow so$, $lh \rightarrow so$ and $hh \rightarrow lh$, can

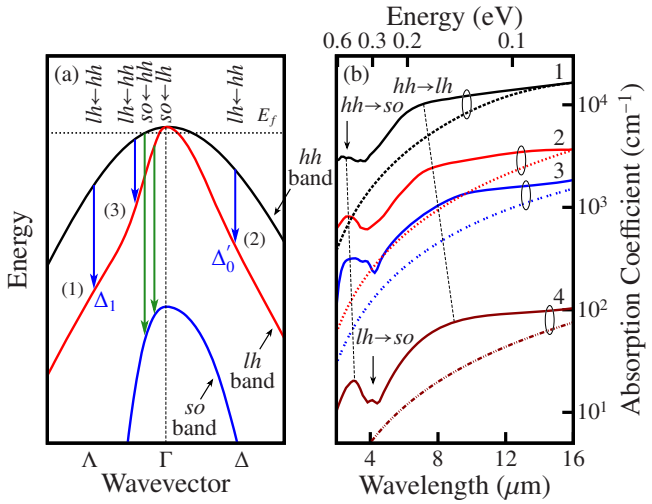

FIG. 1. (Color online) (a) Schematic of the valence-band structure along the direction of $\langle 111\rangle(\Lambda)$ and $\langle 100\rangle(\Delta)$. Various IVBA transitions are indicated. The (1), (2), and (3) represent *lh-hh* transitions at different wave vectors. The Fermi level is calculated for 3×10^{18} cm^{-3} *p*-doped GaAs at 80 K. (b) Measured room-temperature absorption spectra of *p*-GaAs compared with the calculated FCA curves plotted by dashed lines. Also shown is data from Refs. 3 (curves 1) and 13 (curve 4); the doping levels for curves 1–4 are 2.7×10^{19} cm^{-3}, 8.0×10^{18} cm^{-3}, 3.0×10^{18} cm^{-3}, and 2.7×10^{17} cm^{-3}, respectively.

a)Electronic mail: uperera@gsu.edu.

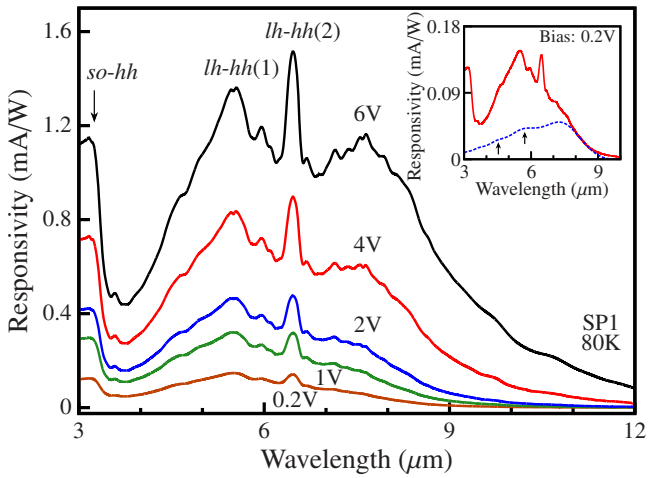

FIG. 2. (Color online) The 80 K responsivity spectra of SP1 at different bias. The inset shows a comparison with modeled responsivity (dashed line) at 0.2 V bias with FCA contribution alone. Peaks indicated by arrows are interference modes of the cavity, which consists of *p*-GaAs/AlGaAs periodic layers. The portion above the FCA curve is ascribed to IVBA contribution, specifically the *lh-hh* transitions for 4–8 μm range.

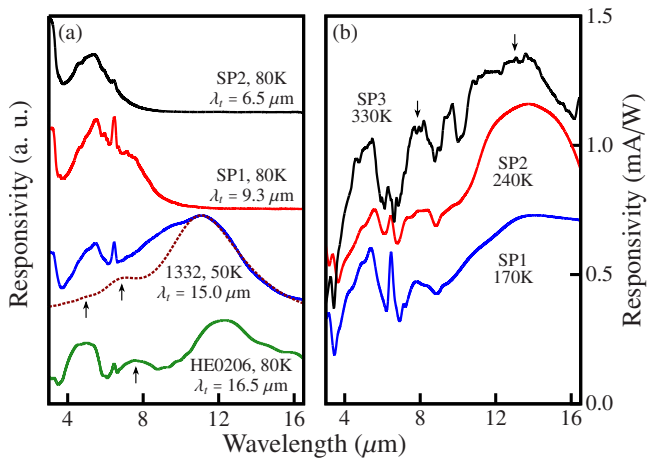

FIG. 3. (Color online) (a) Spectral response of detectors with varied threshold wavelengths (λ_t). The curves from top to bottom are measured at the bias of 8 V, 2 V, 1 V, and 2 V, respectively. In comparison with the FCA response (dashed line) calculated for the detector 1332, *lh-hh* transitions produce response between 4–10 μm. (b) High-operating-temperature capability was measured on samples SP1, SP2, and SP3 under 0.2 V, 0.3 V, and 3 V, respectively, showing broad range from 4–16.5 μm. The wavelength region above designed threshold is due to a thermal detection mechanism. Cavity interference modes are all marked with the arrows in (a) and (b).

be verified from absorption spectra as shown in Fig. 1(b) with theoretical FCA curves (from transitions occurring within the same band) calculated for comparison. The IVBA appears as on top of FCA lines, where the broad peak around 4–16 μm is due to the *lh-hh* transitions. Hole transitions near the BZ center contribute to the long-wavelength portion, such as the transition (3) corresponding to absorption at 9 μm. Although holes occupying the *hh* band reduces with increasing k, the joint density of states (JDOS) $|\vec{k}\cdot\nabla_k(E_{ki}-E_{kj})|^{-1}$ (i and j represent band indexes) showing singularities due to the parallel feature of *lh* and *hh* bands results in considerable absorption in the short-wavelength range. Those transitions can take place in the $\langle 111\rangle(\Lambda)$ and $\langle 100\rangle \times(\Delta)$ directions as indicated by arrows (1) and (2). Such an absorption feature is promising for infrared detection since both MWIR and LWIR ranges can be covered using a single *p*-GaAs based structure.

Detector structures with varied emitter doping and λ_t, demonstrating the *lh-hh* response, were grown on semi-insulating GaAs substrates. Sample HE0206 consists of 16 periods of 18.8 nm *p*-GaAs emitters doped to 1×10^{17} cm^{-3} and 125 nm undoped $Al_{0.12}Ga_{0.88}As$ barriers. Sample 1332 has 12 periodic units with the same thick emitters and barriers as HE0206 but the emitter doping level is at 3×10^{18} cm^{-3} and the Al fraction of barriers is 0.15. Except for the Al fraction, SP1, SP2, and SP3 have same layer parameters with 30 periods of 18.8 nm-thick 3×10^{18} cm^{-3} *p*-doped GaAs and 60 nm thick undoped $Al_xGa_{1-x}As$ where x=0.28, 0.37, and 0.57, respectively. The *so-hh* transition-based short-wavelength response in samples SP1~3 have been previously reported and discussed.[2] The λ_t of HE0206, 1332 and SP1~3 at 16.5 ± 0.5 μm, 15.0 ± 0.3 μm, 9.3 ± 0.3 μm, 6.5 ± 0.3 μm, and 4.1 ± 0.2 μm, respectively, are referred to operating conditions listed in Fig. 3(a). Spectral response was measured on devices with the active area of 260×260 μm^2 by using a Perkin-Elmer system 2000 Fourier Transform InfraRed (FTIR) spectrometer. A bolometer with known sensitivity is used for background measurements and calibrating the responsivity of detectors.

Figure 2 shows the 80 K spectral responsivity of SP1 at different bias. Generally, the photoemission process determines the escape rate of holes out of the emitter region following an escape cone model.[9] However, with increasing bias, the thermal assisted tunneling contribution will mix in this process deteriorating the model accuracy, which can be seen from the increasing threshold wavelength with bias. Therefore, the FCA responsivity alone was calculated using the escape cone model[9] for a bias up to 1 V under which the internal work function is nearly unchanged and taken from the Arrhenius plot based on dark current measurements. Results show an agreement of measured responsivity with the FCA model curves in the long-wavelength portion and one comparison is plotted in the inset of Fig. 2. When the FCA dominates over the IVBA at longer wavelength, a good matching can be obtained which is shown in Fig. 3(a). Similar FCA response pattern will be expected for higher-bias operation at which tunneling effects become prominent. The *lh-hh* transitions thus have the primary contribution to spectral response in the 4–8 μm range in which the short-wavelength response coincides with the absorption curves [Fig. 1(b)] approaching 4 μm, while the long-wavelength portion is affected by the threshold wavelength. Two peaks determined by their center positions at 5.50 μm and 6.46 μm, respectively, can be resolved. Their corresponding energy values (0.225 V and 0.192 eV, respectively) agree well with reported *lh-hh* separations along the Λ and Δ directions, e.g., $\Delta_1(\Lambda)$=0.224 eV in Ref. 10 and $\Delta_0'(\Delta)$ =0.193 eV in Ref. 11. Therefore, hole transitions at points in $\vec{k}$ space along the Λ and Δ directions [named (1) and (2) in Fig. 1(a), respectively] are the reason for this result. A hole escaping over the potential barrier needs to undergo a photoemission process at the emitter-barrier interface during which its kinetic energy is required to be higher than the barriers following an escape cone in the momentum space. Different photoemission rate can be resulted in terms of the k points on the *lh* band onto which holes are excited, leading to the resolved Δ_1 and Δ_0' peaks in Fig. 2.

TABLE I. List of IVBA response peaks for four detector structures at 80 K except the SP3 which is obtained at 330 K. Peaks are determined through their center positions. Different types of IBVA transitions are indicated in Fig. 1(a).

Sample no.	λ_t (μm)	Emitter doping (cm^{-3})	Transition wavelengths (μm)		
			so-hh	*lh-hh*(1)	*lh-hh*(2)
HE0206	16.5 ± 0.5	1×10^{17}	3.26	4.82	6.45
1332	15.0 ± 0.3	3×10^{18}	3.23	5.50	6.46
SP1	9.3 ± 0.3	3×10^{18}	3.19	5.50	6.46
SP2	6.5 ± 0.3	3×10^{18}	3.20	5.47	6.45
SP3	4.1 ± 0.2	3×10^{18}	3.20	5.45	6.47

Developing detectors in the 4–8 μm range is useful for short-range detection of bright infrared sources such as the proximity fuze that is designed to detonate an explosive device. By using GaAs-based alloys such as GaAsP (Δ_{so}(GaP)=0.08 eV) or GaAsSb (Δ_{so}(GaSb)=0.76 eV), extension of response range to either longer or shorter wavelength is possible as Δ_1 roughly follows the $(2/3)\Delta_{so}$ rule. These characteristics will facilitate the realization of multispectral detection on a single GaAs-based detector.

According to Fig. 1(b), *lh-hh* absorption processes can result in a spectral response longer than the response obtained from detector SP1. The long-wavelength capability was investigated in detectors with varied doping levels and λ_t as shown in Fig. 3(a). A comparison with the model FCA response was made on detector 1332 operating at 1 V bias, indicating *lh-hh* transitions can produce spectral response up to 10 μm. The *lh-hh* IVBA process is rather prominent in terms of similar responsivity features observed in detector HE0206 although its emitters are relatively low doped at 1×10^{17} cm^{-3}. A summarization of observed peaks is listed in Table I. High-operating-temperature capability was measured on detectors SP1, SP2, and SP3 as shown in Fig. 3(b), indicating promising uncooled operation. The range above λ_t could be due to the thermal detection mechanisms.[12] Thermal-related processes such as phonon scattering increase the response time at high temperatures at which enhanced responsivity was observed by using a lower optical-path-difference (OPD) velocity of the FTIR. A minimum OPD velocity below which response is nearly unchanged was thus employed. The peak at ~13 μm is due to the cavity enhancement[9] of the *p*-GaAs/AlGaAs structure. It has been found that the Δ_1 and Δ_0' peaks are almost fixed over the temperature range from 80 K to room temperatures, which is consistent with their previous reported temperature-independent behavior.[10]

The calculated specific detectivities (D^*) for SP1 and SP2 at peak response wavelengths and operating at 80 K and 1 V bias by using the previously described methods[2] are 3.0×10^7 and 1.5×10^9 Jones, respectively. Performance optimization is also possible by improving emitter absorption with higher doping levels [Fig. 1(b)]. However, the scattering effect[12] is another factor needed to be considered for a final optimization. The *lh-hh* transition-based concept presented in this paper builds up the factors including the split-off mechanism and the FCA for GaAs being a platform to realize multi-spectral infrared detection in an internal photoemission detector. In comparison with MCT detectors[4] which have been realized for uncooled operation within the 2–16 μm spectral range and are commercially available, the discussed GaAs-based device will be a viable alternative with the robustness of the III-V material system. Uncooled operation is also possible for this type of device which can be promising for some special applications such as high-intensity detection.

This work was supported in part by the U.S. Army Research Office under Grant No. W911NF-08-1-0448 monitored by Dr. William W. Clark, and in part by the U.S. National Science Foundation under Grant No. ECS-0553051. Authors acknowledge Greggory Rothmeier for help in manuscript preparation.

[1] A. G. U. Perera, S. G. Matsik, P. V. V. Jayaweera, K. Tennakone, H. C. Liu, M. Buchanan, G. Von Winckel, A. Stintz, and S. Krishna, Appl. Phys. Lett. **89**, 131118 (2006).
[2] P. V. V. Jayaweera, S. G. Matsik, A. G. U. Perera, H. C. Liu, M. Buchanan, and Z. R. Wasilewski, Appl. Phys. Lett. **93**, 021105 (2008).
[3] W. Songprakob, R. Zallen, D. V. Tsu, and W. K. Liu, J. Appl. Phys. **91**, 171 (2002).
[4] A. Rogalski, Rep. Prog. Phys. **68**, 2267 (2005).
[5] H. Schneider and H. C. Liu, *Springer Series in Optical Sciences* (Springer, New York, 2007), Vol. 126.
[6] G. Ariyawansa, A. G. U. Perera, G. Huang, and P. Bhattacharya, Appl. Phys. Lett. **94**, 131109 (2009).
[7] H. S. Kim, E. Plis, A. Khoshakhlagh, S. Myers, N. Gautam, Y. D. Sharma, L. R. Dawson, S. Krishna, S. J. Lee, and S. K. Noh, Appl. Phys. Lett. **96**, 033502 (2010).
[8] F. R. Giorgetta, E. Baumann, M. Graf, Q. Yang, C. Manz K. Köhler, H. E. Beere, D. A. Ritchie, E. Linfield, A. G. Davies, Y. Fedoryshyn, H. Jäckel, M. Fischer, J. Faist, and D. Hofstetter, IEEE J. Quantum Electron. **45**, 1039 (2009).
[9] D. G. Esaev, M. B. M. Rinzan, S. G. Matsik, and A. G. U. Perera, J. Appl. Phys. **96**, 4588 (2004).
[10] P. Lautenschlager, M. Garriga, S. Logothetidis, and M. Cardona, Phys. Rev. B **35**, 9174 (1987).
[11] S. Zollner, J. Appl. Phys. **90**, 515 (2001).
[12] S. G. Matsik, P. V. V. Jayaweera, A. G. U. Perera, K. K. Choi, and P. Wijewarnasuriya, J. Appl. Phys. **106**, 064503 (2009).
[13] R. Braunstein and E. Kane, J. Phys. Chem. Solids **23**, 1423 (1962).